




Communication

Trace Metal Levels and Nutrient Characteristics of Crude Oil-Contaminated Soil Amended with Biochar–Humus Sediment Slurry

Nnanake-Abasi O. Offiong^{1,2,3,*}, Edu J. Inam^{1,2,*}, Helen S. Etuk^{1,2}, Godwin A. Ebong^{1,2}, Akwaowo I. Inyangudoh^{1,2} and Francis Addison³

¹ International Centre for Energy and Environmental Sustainability Research (ICEESR), University of Uyo, Uyo 520001, Nigeria; helenetuk.etuk@yahoo.com (H.S.E.); g_ebong@yahoo.com (G.A.E.); akwaowoinyangudoh20@gmail.com (A.I.I.)

² Department of Chemistry, University of Uyo, Uyo 520001, Nigeria

³ College of New Energy and Environment, Jilin University, Changchun 130021, China; francisaddison@yahoo.com

* Correspondence: offiong18@mails.jlu.edu.cn (N.-A.O.O.); eduinam@uniuyo.edu.ng (E.J.I.)

Abstract: Biochar utilization for environmental remediation applications has become very popular. We investigated the trace metal levels and soil nutrient characteristics of a biochar–humus sediment slurry treatment of a simulated crude oil-contaminated soil in the present work. The results revealed that biochar prepared at moderate pyrolysis temperature (500 °C) could still retain a significantly higher nutrient content than those prepared at high temperatures (700 and 900 °C). Despite the suitability for soil treatment, one-pot treatment studies seem not to be very effective for monitoring trace metal sorption to biochar because trace metals do not biodegrade and remain in the system.

Keywords: trace metals; oil spill; nutrients; biochar; humus sediment slurry; remediation



Citation: Offiong, N.-A.O.; Inam, E.J.; Etuk, H.S.; Ebong, G.A.; Inyangudoh, A.I.; Addison, F. Trace Metal Levels and Nutrient Characteristics of Crude Oil-Contaminated Soil Amended with Biochar–Humus Sediment Slurry. *Pollutants* **2021**, *1*, 119–126. <https://doi.org/10.3390/pollutants1030010>

Academic Editors: Salvatore Barreca and Santino Orecchio

Received: 13 May 2021
Accepted: 5 June 2021
Published: 23 June 2021

Publisher's Note: MDPI stays neutral with regard to jurisdictional claims in published maps and institutional affiliations.



Copyright: © 2021 by the authors. Licensee MDPI, Basel, Switzerland. This article is an open access article distributed under the terms and conditions of the Creative Commons Attribution (CC BY) license (<https://creativecommons.org/licenses/by/4.0/>).

1. Introduction

Soil pollution by crude oil spills still constitutes a major environmental problem in many countries where oil exploration is the mainstay of the economy [1]. The introduction of potentially toxic trace metals and organic contaminants into the environment is considered a threat to human and environmental health [2–5].

Due to their resistance to natural breakdown, heavy metals are among the most persistent contaminants in the environment [6]. Except in acidic pH conditions, trace metals are less soluble in water and tend to adsorb on particulates. As a result, increased mobility is expected in acidic soils. Once released into the environment, trace metals can also be bioaccumulated by living organisms through dermal or foliage absorption, root intake, and other feeding habits. The major concerns over exposure to trace metals include the deleterious effects they have on human and environmental health. These include possible cancer, cardiovascular diseases, and neurological disorders [7]. Consequently, trace metal pollution via oil spills has been an important topic of investigation [8–10].

Due to greater environmental awareness and stricter environmental regulations in these countries, many attempts have been made to remediate such polluted sites. Among the methods adopted include isolation and containment, mechanical separation, pyrometallurgical separation, biochemical processes, phytoremediation, soil flushing, soil washing, electrokinetics, and vitrification [11–13]. A major setback of most of these remediation approaches is that they are devoid of soil fertility restoration aspects [1]. This is a key aspect of environmental remediation for acidic soils (ultisols) which are generally characterized by low nutrient levels [14]. There has been, and there is still, a growing interest in nutrient recovery from waste biomass for remediation purposes while addressing soil fertility issues.

Raw, pyrolyzed, and ashed biomass (activated carbon or biochar) materials are adequate for the biogeochemical cycling of various compounds and nutrients in soils [15–21]. For this reason, biochar and other ashed biomass have been screened for trace metal and organic contaminant remediation applications with low cost and soil nutrient restoration agenda [22–32]. Composting of biochar with other organic wastes has also been investigated [33]. Previous investigations have shown that sediment bioslurry and composts could effectively attenuate contaminants in soil [34–36]. However, it is not clear how biochar in such composts could affect soil trace metal levels and nutrient characteristics in the presence of other environmental stressors such as crude oil contamination. Therefore, the objective of the present study was to investigate the physicochemical characteristics, nutrients, and trace metal distribution in a simulated crude oil-contaminated soil (ultisol) amended with biochar–humus sediment slurry.

2. Materials and Methods

Untreated Bonny Light crude oil was provided by the Shell Petroleum Development Company of Nigeria. Humic acid (HA) was purchased from Sigma Aldrich (Cambridge, UK). Humus sediment (HS) was sampled from a humus freshwater ecosystem in Niger Delta, Nigeria, which has been fully characterized in previous studies [34]. The biochar samples were prepared from air-dried sewage sludge at three different pyrolysis temperatures (500 °C (BC500), 700 °C (BC700), and 900 °C (BC900)) under limited oxygen conditions. More details about sewage sludge sampling have been presented in a previous report [29]. Briefly, laboratory simulations were carried out in wooden boxes with small perforated holes. Each of the boxes contained different amounts of prepared biochar–humus sediment slurry and crude oil volumes. Briefly, the following simulations were set-up: A (blank: soil (4 kg) + crude oil (120 mL)); B (soil (4 kg) + crude oil (120 mL) + HA (5 g)); C (soil (4 kg) + crude oil (120 mL) + HS (5 g) + HA (5 g) + biochar (5 g)); and D (soil (4 kg) + crude oil (120 mL) + HA (5 g) + HS (5 g)). Soil microcosm batch experiments were set up according to a previous report and monitored with BC500 treatment because it recorded favorable physicochemical parameters after a preliminary analysis [34].

Analysis of soil, sewage sludge, biochars, and composites were based on standard analytical protocols adopted from available literature [37–39].

2.1. Determination of pH

Exactly 20 g of an air-dried sample was placed into a 100 mL beaker. Exactly 40 mL of distilled water was added, stirred, and allowed to stand for 30 min. The pH electrodes were then inserted into the partly settled suspension, and the results were read.

2.2. Determination of Organic Carbon Content

Precisely 0.5 g of a air-dried, homogenized, and sieved sample was placed in a 250 mL conical flask. Thereafter, 10 mL of standard potassium dichromate ($K_2Cr_2O_7$, 0.083 M) solution was added and swirled to mix. To the resulting solution, 15 mL concentrated H_2SO_4 was added, and the solution was swirled gently to mix. Exactly 100 mL of distilled water was added and allowed to stand for 30 min. The solution was swirled again to mix and 5 drops of ferroin indicator were added. The resulting solution was titrated with 0.2 M ferrous ammonium sulfate to the endpoint at which the color changed from blue-green to violet red. The procedure was repeated for the blank samples. Organic carbon content was calculated using Equations (1) and (2):

$$\text{Organic carbon (mg/g)} = [18 \times C \times V \times (1 - V_1/V_2)]/M \quad (1)$$

where C = concentration in mol/L of potassium dichromate, V = volume of potassium dichromate, V_1 = volume of titrant used up in the sample determination, V_2 = volume of titrant used up in the blank determination, and M = weight of sample used.

$$\text{Organic carbon (\%)} = (\text{organic carbon (mg/g)})/10 \quad (2)$$

2.3. Determination of Cation Exchange Capacity (CEC)

The cation exchange capacity (CEC) was determined by a modified ammonium acetate displacement method [40]. Five grams of a sample was placed in a 100 mL polyethylene bottle. Exactly 25 mL of ammonium acetate solution was added. The mixture was shaken for 1 h. The supernatant was filtered into a 100 mL volumetric flask through a filter paper held in a funnel. Then, 20 mL of ethanol (95%) was added and shaken again. The mixture was allowed to settle, followed by filtration into a 100 mL flask as before. The sample was then mixed with 25 mL KCl (pH 2.5) solution and shaken for 30 min followed by filtration into a 100 mL volumetric flask. The sample on the filter was leached with small portions of KCl solution into the flask and filled to the mark. An aliquot of 50 mL was transferred into a 250 mL round-bottom flask and diluted with 50 mL of water. The concentration of NH_4^+ in the extracting solution was determined by titration according to Equation (3):

$$\text{NH}_4\text{-N (mg/kg)} = 140 \times F \times V/M \quad (3)$$

where V = volume of titrant (0.005 M H_2SO_4) used (mL), M = weight of sample (g), and F = inverse of the fraction of extract taken for distillation (i.e., $F = 1/0.5 = 2$).

The computed value obtained from Equation (3) was divided by the atomic mass of nitrogen (14) in order to convert to meq/kg. To obtain the CEC, the result was further converted to meq (100 g)⁻¹ (Equation (4)):

$$\text{CEC [meq(100 g)}^{-1}] = \text{NH}_4\text{-H [meq(100 g)}^{-1}] = F \times V/M \quad (4)$$

2.4. Determination of Nitrogen Content

The Kjeldahl method was used to determine the total nitrogen content in the samples as described by Radojevic and Bashkin [39]. Briefly, 5 g of an air-dried, sieved (2 mm) sample was placed in the Kjeldahl digestion flask. Five grams of K_2SO_4 and 1 g of copper sulfate were added. Exactly 10 mL of concentrated H_2SO_4 was added while being swirled, followed by gentle heating for 3 h at 380 °C. After cooling, about 40 mL of water was added, and the sample was allowed to stand for few minutes until the particles settled to the bottom. The digest was transferred to a clean macro Kjeldahl flask (750 mL). Exactly 150 mL of 1 M NaOH solution was added after the Kjeldahl distillation apparatus was set up. Exactly 150 mL of the distillate was collected, and the $\text{NH}_3\text{-N}$ content was determined by titration with 0.01 M standard H_2SO_4 . The color change at the endpoint was from green to pink. The total nitrogen content was calculated from Equation (5):

$$\% \text{ N} = (T \times M \times 14 \times 100)/W \quad (5)$$

where C = concentration of $\text{NH}_3\text{-N}$ in the distillate solution (mg/L), V = volume of distillate solution after dilution (mL), and M = weight of sample (g).

2.5. Determination of Phosphorus Content

Five grams of an air-dried sample was placed into an appropriate bottle and 200 mL of acetic acid (2.5%, v/v) was added. The mixture was shaken for 1 h on a rotary shaker. The mixture was filtered into polyethylene bottles using Whatman No. 40 filter paper. The first 5–10 mL was discarded. About 10 mL of the sample extract was pipetted into a 50 mL volumetric flask. Exactly 5 drops of 0.25% *p*-nitroresol were added. The solution was adjusted to pH 7 using 5 M HCl or 5 M NaOH, as the case may be. Distilled water was added to bring the solution to 40 mL, and 200 mL of Murphy–Riley reagent was added and thoroughly mixed. Absorbance was measured at 880 nm in a 1 cm cell using UV/Vis spectrophotometer. The concentration of phosphorus was determined by extrapolation from the calibration graph of absorbance against standard concentration of phosphate.

2.6. Determination of Trace Metals

Five grams of a sample was placed in a Teflon beaker, and a mixture of 4 M HNO₃ (10 mL) and H₂O₂ (20 mL) was gradually added. The mixture was left to digest under reflux on a hot sand bath. After refluxing for 1 h, the samples were removed, transferred to an evaporating dish, and left to evaporate to dryness on a hot plate. The samples were then removed and treated with 6 M HCl (5 mL) and made up to mark in a 100 mL volumetric flask with deionized water. Trace metals were determined by atomic absorption spectrophotometry (AAS).

2.7. Determination of Potassium Content

Potassium content in the soil, sediment, and sludge samples was determined by flame photometry. Briefly, about 5 g of a sieved and air-dried sample was placed in a conical flask. Exactly 50 mL of 0.5 M ammonium acetate/acetic acid solution was added and shaken for 30 min. The resulting sample was left to stand for a while, after which it was filtered. The filtrate was read on the flame photometer to determine potassium.

2.8. Data Analysis

Descriptive statistics were performed using Excel 2007 spreadsheet while multivariate analyses and ANOVA were done using the SPSS statistical software package Version 20.0 with the level of significance set at $p < 0.05$.

3. Results

The results of pH, total organic carbon (TOC), total nitrogen, total phosphorus, potassium, and cation exchange capacity for the blank soil, sewage sludge, humus sediment, treated soils, and pyrolyzed sludge are presented in Tables 1 and 2. The pH varied across samples with the pyrolyzed samples showing more alkalinity (pH > 7). The reverse was observed for TOC, with pyrolyzed samples recording the lowest values (3.51%). Treatment of the simulated contaminated soils with biochar composites tended to reduce acidity and increase nutrient (nitrogen, phosphorus, and potassium (NPK)) contents of the soils.

Table 1. Variation in physicochemical and nutrient characteristics of biochars prepared at different temperatures.

Parameter	BC500	BC700	BC900
pH	8.10 ± 0.22	9.20 ± 0.32	9.10 ± 1.10
Total organic carbon (%)	3.51 ± 0.02	2.3 ± 0.03	2.8 ± 0.21
Total nitrogen (%)	0.73 ± 0.01	0.52 ± 0.02	0.24 ± 0.01
Total phosphorus (%)	0.78 ± 0.01	0.07 ± 0.00	0.05 ± 0.01
Potassium (mg/kg)	35.33 ± 5.34	42.22 ± 7.55	26.17 ± 5.77
CEC (meq/100 g)	0.17	0.17	0.14

Table 2. Preliminary characteristics of soil (blank), sewage sludge, humus sediment, biochar prepared at 500 °C, and treated soils.

Parameter	Soil Blank	Sewage Sludge	Humus Sediment	BC500	Contaminated Soil (A)	Treated Soils *
pH	6.0 ± 0.36	5.8 ± 0.12	6.0 ± 0.44	8.10 ± 0.22	6.8 ± 0.02	7.6 ± 0.20
Total organic carbon (%)	4.05 ± 1.15	4.63 ± 0.50	10.17 ± 1.25	3.51 ± 0.02	5.5 ± 1.12	2.79 ± 0.55
Total nitrogen (%)	0.01 ± 0.00	4.16 ± 0.13	1.20 ± 0.08	0.73 ± 0.01	0.02 ± 0.00	3.88 ± 0.09
Total phosphorus (%)	0.07 ± 0.02	3.63 ± 0.10	24.11 ± 2.90	0.78 ± 0.01	0.08 ± 0.02	4.43 ± 0.60
Potassium (mg/kg)	7.47 ± 0.12	64.81 ± 6.33	15.80 ± 3.11	35.33 ± 5.34	6.34 ± 0.55	13.66 ± 3.60
CEC (meq/100 g)	0.46	21.02	-	0.17	-	-

* treated with BC500; CEC = cation exchange capacity.

Preliminary analysis of materials and soil samples revealed varying levels of trace metals, as presented in Table 3. The blank soil was found to contain the highest chromium level (0.83 ± 0.04 mg/kg) and had a cadmium level of 0.01 mg/kg. In the contaminated soil, the chromium level was 0.54 mg/kg, while the cadmium level remained unchanged compared

to the blank soil. However, in the biochar-treated soil, lead and copper were reduced to 0.07 and 0.18 mg/kg, respectively, while the cadmium level remained at 0.01 mg/kg.

The results of the trace metals in soils treated with different amounts of biochar are presented in Table 4, and the results obtained from soils under different levels of crude oil contamination are presented in Table 5. The trace metal levels varied without a specific trend. However, the highest levels were recorded for Zn in all cases, while low levels were recorded for Cr and Cd.

Table 3. Levels of trace metals (mg/kg) in sludge, humus sediment, and contaminated and treated soils.

Trace Metals	Blank Soil	Humus Sediment	Contaminated Soil (Sample A)	Sewage Sludge	Pyrolyzed Sludge			Treated Soil *
					BC500	BC700	BC900	
Zn	0.41 ± 0.02	0.33 ± 0.13	0.36 ± 0.03	0.17 ± 0.00	0.23 ± 0.30	1.10 ± 1.50	0.27 ± 0.23	0.48 ± 0.08
Pb	0.13 ± 0.01	0.15 ± 0.06	0.10 ± 0.00	0.13 ± 0.02	0.10 ± 0.09	0.12 ± 0.02	0.10 ± 0.04	0.07 ± 0.01
Cr	0.83 ± 0.04	0.01 ± 0.00	0.54 ± 0.13	0.01 ± 0.00	0.05 ± 0.05	0.07 ± 0.02	0.06 ± 0.06	0.60 ± 0.01
Cd	0.01 ± 0.00	0.01 ± 0.00	0.01 ± 0.00	0.12 ± 0.03	0.07 ± 0.10	0.07 ± 0.10	0.07 ± 0.10	0.01 ± 0.00
Cu	0.20 ± 0.10	0.22 ± 0.03	0.14 ± 0.02	0.09 ± 0.00	0.06 ± 0.07	0.38 ± 0.50	0.08 ± 0.10	0.18 ± 0.04

* Soil treated with BC500.

Table 4. Variation of trace metal levels (mg/kg) in relation to biochar/humus sediment mixture concentration.

Trace Metals	Concentration of Biochar/Humus Sediment Mixture				
	15 g ^a	20 g ^b	25 g ^c	35 g ^d	60 g ^e
Zn	2.94 ± 1.00	1.66 ± 0.50	9.10 ± 2.49	5.34 ± 0.47	10.78 ± 0.80
Pb	0.23 ± 0.11	0.19 ± 0.08	0.17 ± 0.10	0.51 ± 0.15	0.25 ± 0.06
Cr	0.16 ± 0.06	0.13 ± 0.01	0.10 ± 0.01	0.20 ± 0.11	0.16 ± 0.08
Cd	0.11 ± 0.00	0.07 ± 0.00	0.11 ± 0.02	0.22 ± 0.02	0.12 ± 0.10
Cu	0.37 ± 0.15	0.39 ± 0.01	0.12 ± 0.00	1.00 ± 0.00	1.37 ± 0.05

^a: 5 g of biochar and 10 g of humus sediment; ^b: 10 g of biochar and 10 g of humus sediment; ^c: 15 g of biochar and 10 g of humus sediment;

^d: 25 g of biochar and 10 g of humus sediment; ^e: 50 g of biochar and 10 g of humus sediment.

Table 5. Variation of trace metal levels (mg/kg) in relation to crude oil contamination level.

Trace Metals	Level of Contamination (Volume of Crude Oil Spiked)				
	120 mL ^a	200 mL ^b	250 mL ^c	300 mL ^d	500 mL ^e
Zn	15.38 ± 3.50	14.34 ± 2.40	9.63 ± 1.80	12.37 ± 4.22	9.59 ± 3.15
Pb	0.69 ± 0.05	3.60 ± 1.20	2.14 ± 0.00	2.14 ± 0.13	0.30 ± 0.11
Cr	0.29 ± 0.01	0.99 ± 0.10	0.59 ± 0.02	0.59 ± 0.47	0.16 ± 0.02
Cd	0.43 ± 0.01	2.28 ± 0.30	1.19 ± 0.30	0.22 ± 0.32	0.10 ± 0.01
Cu	1.61 ± 0.20	2.11 ± 1.00	1.52 ± 0.50	1.42 ± 0.62	1.15 ± 0.25

^a: 5 g of biochar and 10 g of humus sediment; ^b: 10 g of biochar and 10 g of humus sediment; ^c: 15 g of biochar and 10 g of humus sediment;

^d: 25 g of biochar and 10 g of humus sediment; ^e: 50 g of biochar and 10 g of humus sediment.

4. Discussion

The pH, TOC, total nitrogen, and phosphorus content were generally low in the blank soil but were higher in the sewage sludge and humus sediment. These parameters were also low in the biochars obtained after pyrolysis of sludge (Table 2). The observed decrease in nutrient content in pyrolyzed sludge (biochar) as pyrolysis temperature increased is due to the decomposition of nitrate, ammonium salts and phosphate salts [41]. Cation exchange capacity (CEC) was highest for the sewage sludge but low in biochars (Table 1). Although high CEC generally accounts for retention of nutrient cations [42], this aspect that is required for microbial growth could be augmented by high nitrogen, phosphorous, and potassium (NPK) content in the humus sediment (Table 2).

Furthermore, variation in pyrolysis temperature regulates the properties of biochars. While some parameters such as the yield, polarity, H%, and O% would decrease, the pH, C%, ash, aromaticity, and surface area would increase [43]. However, there may be

some variations in the degree of dominance of these parameters across different feedstocks and pyrolysis temperatures. For instance, the total nitrogen content (2.3%) reported by Hossain et al. [44] for biochar produced at 550 °C was higher than the values obtained in this study. The authors also reported relatively high phosphorus content (1100 mg/kg). Similarly, Zielinska et al. [45] observed an increase in pH from low (500 °C) to high (700 °C) pyrolysis temperature: 7.01–7.39 and 12.23–13.10, respectively. For the same temperature range, they reported a decrease in the nitrogen content: 2.22–3.95% and 1.88–2.92%, respectively. Yuan et al. [19] reported very high NPK values in thousand units with K decreasing with an increase in pyrolysis temperature, from 7470 to 16,600 mg/kg at 300 and 700 °C pyrolysis temperatures, respectively. In contrast, the potassium content did not show any consistent trend in the present work. The only plausible explanation for this contrasting result is the possible formation of complexes of volatile potassium compounds that could evaporate at higher temperatures [46]. On the other hand, Hossain et al. [47] reported low N and moderate P content in wastewater sludge biochar. Thus, it is possible to have different magnitudes of NPK ratios for a given biochar feedstock pyrolyzed at different temperatures. However, it is not clear if similar NPK ratios could be obtained for a given feedstock when other production parameters are kept constant. Overall, the nutrient contents of biochars reported in the present study are within the lower ranges compared to those in other studies. The results in Table 2 reveal that the biochar–humus sediment mixture affected the physicochemical and nutrient characteristics of treated soils. For example, potassium, total nitrogen, and phosphorus contents increased in treated soils. The pH was moderated towards neutral level, considering that the soils were originally acidic and would neutralize on amendment with alkaline ashed biomass.

Generally, trace metals were in similar ranges across the blank soils, sewage sludge, pyrolyzed sludge, and treated soil. For soil treatment, one-pot treatment studies seem not to be very effective for monitoring trace metal sorption to biochar because trace metals do not biodegrade and remain in the system. Monitoring trace metals in such systems is better done by using an external bioaccumulator for biomonitoring [48].

5. Conclusions

We monitored nutrient parameters (N, P, K) and trace metal levels in crude oil-contaminated soils amended with biochar–humus sediment slurry. The results revealed varying levels of trace metals and nutrient contents in the treated soils. Pyrolysis temperature influences the nutrient retention capability of biochar. Specifically, biochar pyrolyzed at 500 °C retained more nutrients compared to those pyrolyzed at 700 and 900 °C. Furthermore, it was observed that potassium, total nitrogen, and phosphorus contents increased in amended soil. However, trace metal levels either slightly increased or were unchanged in the amended soils. We conclude that monitoring trace metals in such systems is better done by using an external bioaccumulator for biomonitoring since metals do not degrade.

Author Contributions: Conceptualization, E.J.I. and N.-A.O.O.; methodology, N.-A.O.O.; formal analysis, N.-A.O.O.; investigation, N.-A.O.O.; resources, E.J.I. and N.-A.O.O.; data curation, N.-A.O.O.; writing—original draft preparation, N.-A.O.O.; writing—review and editing, E.J.I., H.S.E., G.A.E., A.I.I., and F.A.; supervision, E.J.I. and H.S.E.; funding acquisition, N.-A.O.O. and E.J.I. All authors have read and agreed to the published version of the manuscript.

Funding: Funding support for this research was received from Shell Petroleum Development Company of Nigeria (SPDC) in 2015–2016.

Conflicts of Interest: The authors declare no conflict of interest.

References

1. Dominguez-Rodriguez, V.I.; Adams, R.H.; Vargas-Almeida, M.; Zavala-Cruz, J.; Romero-Frasca, E. Fertility Deterioration in a Remediated Petroleum-Contaminated Soil. *Int. J. Environ. Res. Public Health* **2020**, *17*, 382. [[CrossRef](#)] [[PubMed](#)]
2. Emoyan, O.O.; Peretiemo-Clarke, B.O.; Tesi, G.O.; Adjerese, W.; Ohwo, E. Occurrence, Origin and Risk Assessment of Trace Metals Measured in Petroleum Tank-farm Impacted Soils. *Soil Sediment Contam.* **2020**, *30*, 384–408. [[CrossRef](#)]

3. Lassalle, G.; Credoza, A.; Hedacq, R.; Fabre, S.; Dubucq, D.; Elger, A. Assessing Soil Contamination Due to Oil and Gas Production Using Vegetation Hyperspectral Reflectance. *Environ. Sci. Technol.* **2018**, *52*, 1756–1764. [[CrossRef](#)] [[PubMed](#)]
4. Offiong, N.A.O.; Inam, E.J.; Etuk, H.S.; Essien, J.P. Current status and challenges of remediating petroleum-derived PAHs in soils: Nigeria as a case study for developing countries. *Remediation J.* **2019**, *30*, 65–75. [[CrossRef](#)]
5. Ogunlaja, A.; Ogunlaja, O.O.; Okewole, D.M.; Morenikeji, O.A. Risk assessment and source identification of heavy metal contamination by multivariate and hazard index analyses of a pipeline vandalised area in Lagos State, Nigeria. *Sci. Total Environ.* **2019**, *651*, 2943–2952. [[CrossRef](#)]
6. Iordache, M.; Iordache, A.M.; Sandru, C.; Voica, C. Assessment of heavy metals pollution in sediments from reservoirs of the Olt River as tool for environmental risk management. *Rev. Chim.* **2019**, *70*, 4153–4162. [[CrossRef](#)]
7. Bartha, S.; Taut, I.; Goji, G.; Andravlad, I.; Dinulică, F. Heavy metal content in polyfloralhoney and potential health risk. A case study of Coșea Mică, Romania. *Int. J. Environ. Res. Public Health* **2020**, *17*, 1507. [[CrossRef](#)]
8. Onojake, M.C.; Frank, O. Assessment of heavy metals in a soil contaminated by oil spill: A case study in Nigeria. *Chem. Ecol.* **2013**, *29*, 246–254. [[CrossRef](#)]
9. Kumar, A.; Ramanathan, A.L.; Prasad, M.B.K.; Datta, D.; Kumar, M.; Sappal, S.M. Distribution, enrichment, and potential toxicity of trace metals in the surface sediments of Sundarban mangrove ecosystem, Bangladesh: A baseline study before Sundarban oil spill of December, 2014. *Environ. Sci. Pollut. Res.* **2016**, *23*, 8985–8999. [[CrossRef](#)]
10. Hussain, T.; Gondal, M.A. Monitoring and assessment of toxic metals in Gulf War oil spill contaminated soil using laser-induced breakdown spectroscopy. *Environ. Monit. Assess.* **2008**, *136*, 391–399. [[CrossRef](#)]
11. Liu, L.; Li, W.; Song, W.; Guo, M. Remediation techniques for heavy metal-contaminated soils: Principles and applicability. *Sci. Total Environ.* **2018**, *633*, 206–219. [[CrossRef](#)]
12. Mulligan, C.N.; Yong, R.N.; Gibbs, B.F. Remediation technologies for metal-contaminated soils and groundwater: An evaluation. *Eng. Geol.* **2001**, *60*, 193–207. [[CrossRef](#)]
13. Peng, W.; Li, X.; Xiao, S.; Fan, W. Review of remediation technologies for sediments contaminated by heavy metals. *J. Soils Sediments* **2018**, *18*, 1701–1719. [[CrossRef](#)]
14. Peng, X.; Ye, L.L.; Wang, C.H.; Zhou, H.; Sun, B. Temperature- and duration-dependent rice straw-derived biochar: Characteristics and its effects on soil properties of an Ultisol in southern China. *Soil Tillage Res.* **2011**, *112*, 159–166. [[CrossRef](#)]
15. Islam, M.; Halder, M.; Siddique, M.A.B.; Razir, S.A.A.; Sikder, S.; Joardar, J.C. Banana peel biochar as alternative source of potassium for plant productivity and sustainable agriculture. *Int. J. Recycl. Org. Waste Agric.* **2019**, *8*, 407–413. [[CrossRef](#)]
16. Puga, A.P.; Grutzmacher, P.; Cerri, C.E.P.; Ribeirinho, V.S.; Andrade, C.A. Biochar-based nitrogen fertilizers: Greenhouse gas emissions, use efficiency, and maize yield in tropical soils. *Sci. Total Environ.* **2020**, *704*, 135375. [[CrossRef](#)]
17. Anderson, C.R.; Condron, L.M.; Clough, T.J.; Fiers, M.; Stewart, A.; Hill, R.A.; Sherlock, R.R. Biochar induced soil microbial community change: Implications for biogeochemical cycling of carbon, nitrogen and phosphorus. *Pedobiologia* **2011**, *54*, 309–320. [[CrossRef](#)]
18. El-Naggar, A.; Lee, S.S.; Rinklebe, J.; Farooq, M.; Song, H.; Sarmah, A.K.; Zimmerman, A.R.; Ahmad, M.; Shaheen, S.M.; Ok, Y.S. Biochar application to low fertility soils: A review of current status, and future prospects. *Geoderma* **2019**, *337*, 536–554. [[CrossRef](#)]
19. Yuan, H.; Lu, T.; Wang, Y.; Chen, Y.; Lei, T. Sewage sludge biochar: Nutrient composition and its effect on the leaching of soil nutrients. *Geoderma* **2016**, *267*, 17–23. [[CrossRef](#)]
20. Clough, T.; Condron, L.; Kammann, C.; Müller, C. A Review of biochar and soil nitrogen dynamics. *Agronomy* **2013**, *3*, 275–293. [[CrossRef](#)]
21. Gul, S.; Whalen, J.K. Biochemical cycling of nitrogen and phosphorus in biochar-amended soils. *Soil Biol. Biochem.* **2016**, *103*, 1–15. [[CrossRef](#)]
22. Li, G.; Chen, F.; Jia, S.; Wang, Z.; Zuo, Q.; He, H. Effect of biochar on Cd and pyrene removal and bacteria communities variations in soils with culturing ryegrass (*Lolium perenne* L.). *Environ. Pollut.* **2020**, *265*, 114887. [[CrossRef](#)]
23. Mukome, F.N.D.; Buelow, M.C.; Shang, J.; Peng, J.; Rodriguez, M.; Mackay, D.M.; Pignatello, J.J.; Sihota, N.; Hoelen, T.P.; Parikh, S.J. Biochar amendment as a remediation strategy for surface soils impacted by crude oil. *Environ. Pollut.* **2020**, *265*, 115006. [[CrossRef](#)]
24. Nigam, N.; Yadav, V.; Mishra, D.; Karak, T.; Khare, P. Biochar amendment alters the relation between the Pb distribution and biological activities in soil. *Int. J. Environ. Sci. Technol.* **2019**, *16*, 8595–8606. [[CrossRef](#)]
25. Pan, M. Biochar adsorption of antibiotics and its implications to remediation of contaminated soil. *Water Air Soil Pollut.* **2020**, *231*. [[CrossRef](#)]
26. Park, J.H.; Choppala, G.K.; Bolan, N.S.; Chung, J.W.; Chuasavathi, T. Biochar reduces the bioavailability and phytotoxicity of heavy metals. *Plant Soil* **2011**, *348*, 439–451. [[CrossRef](#)]
27. Park, J.H.; Lamb, D.; Paneerselvam, P.; Choppala, G.; Bolan, N.; Chung, J.W. Role of organic amendments on enhanced bioremediation of heavy metal(loid) contaminated soils. *J. Hazard. Mater.* **2011**, *185*, 549–574. [[CrossRef](#)]
28. Ramtahal, G.; Umaharan, P.; Hanuman, A.; Davis, C.; Ali, L. The effectiveness of soil amendments, biochar and lime, in mitigating cadmium bioaccumulation in *Theobroma cacao* L. *Sci. Total Environ.* **2019**, *693*, 133563. [[CrossRef](#)]
29. Wei, Z.; Wang, J.J.; Gaston, L.A.; Li, J.; Fultz, L.M.; DeLaune, R.D.; Dodla, S.K. Remediation of crude oil-contaminated coastal marsh soil: Integrated effect of biochar, rhamnolipid biosurfactant and nitrogen application. *J. Hazard. Mater.* **2020**, *396*, 122595. [[CrossRef](#)]

30. Wu, S.; He, H.; Inthapanya, X.; Yang, C.; Lu, L.; Zeng, G.; Han, Z. Role of biochar on composting of organic wastes and remediation of contaminated soils—a review. *Environ. Sci. Pollut. Res.* **2017**, *24*, 16560–16577. [[CrossRef](#)]
31. Yang, B.; Luo, W.; Wang, X.; Yu, S.; Gan, M.; Wang, J.; Liu, X.; Qiu, G. The use of biochar for controlling acid mine drainage through the inhibition of chalcopyrite biodissolution. *Sci. Total Environ.* **2020**, *737*, 139485. [[CrossRef](#)] [[PubMed](#)]
32. Zhang, Y.; Zhao, C.; Chen, G.; Zhou, J.; Chen, Z.; Li, Z.; Zhu, J.; Feng, T.; Chen, Y. Response of soil microbial communities to additions of straw biochar, iron oxide, and iron oxide-modified straw biochar in an arsenic-contaminated soil. *Environ. Sci. Pollut. Res.* **2020**, *27*, 23761–23768. [[CrossRef](#)] [[PubMed](#)]
33. Sanchez-Monedero, M.A.; Cayuela, M.L.; Roig, A.; Jindo, K.; Mondini, C.; Bolan, N. Role of biochar as an additive in organic waste composting. *Bioresour. Technol.* **2018**, *247*, 1155–1164. [[CrossRef](#)] [[PubMed](#)]
34. Offiong, N.-A.O.; Inam, E.J.; Etuk, H.S.; Essien, J.P.; Ofor, U.A.; Una, C.C. Biochar and humus sediment mixture attenuates crude oil-derived PAHs in a simulated tropical ultisol. *SN Appl. Sci.* **2020**, *2*. [[CrossRef](#)]
35. Robles-Gonzalez, I.V.; Fava, F.; Poggi-Varaldo, H.M. A review on slurry bioreactors for bioremediation of soils and sediments. *Microb. Cell Fact.* **2008**, *7*, 5. [[CrossRef](#)]
36. Talley, J.W.; Ghosh, U.; Tucker, S.G.; Furey, J.S.; Luthy, R.G. Particle-scale understanding of the bioavailability of PAHs in sediment. *Environ. Sci. Technol.* **2002**, *36*, 477–483. [[CrossRef](#)]
37. Keith, L.K. *Environmental Sampling and Analysis: A Practical Guide*; Lewis Publishers: Boca Raton, FL, USA, 1991.
38. Christian, G.D. *Analytical Chemistry*, 6th ed.; John Wiley & Sons: Singapore, 2004; p. 828.
39. Radojević, M.; Bashkin, V.N. *Practical Environmental Analysis*, 2nd ed.; Royal Society of Chemistry: London, UK, 2006; p. 457.
40. Gai, X.; Wang, H.; Liu, J.; Zhai, L.; Liu, S.; Ren, T.; Liu, H. Effects of feedstock and pyrolysis temperature on biochar adsorption of ammonium and nitrate. *PLoS ONE* **2014**, *9*, e113888. [[CrossRef](#)]
41. Yuan, H.; Lu, T.; Huang, H.; Zhao, D.; Kobayashi, N.; Chen, Y. Influence of pyrolysis temperature on physical and chemical properties of biochar made from sewage sludge. *J. Anal. Appl. Pyrolysis* **2015**, *112*, 284–289. [[CrossRef](#)]
42. Anyika, C.; Abdul Majid, Z.; Ibrahim, Z.; Zakaria, M.P.; Yahya, A. The impact of biochars on sorption and biodegradation of polycyclic aromatic hydrocarbons in soils—A review. *Environ. Sci. Pollut. Res.* **2015**, *22*, 3314–3341. [[CrossRef](#)]
43. Xiao, X.; Chen, B.; Chen, Z.; Zhu, L.; Schnoor, J.L. Insight into multiple and multilevel structures of biochars and their potential environmental applications: A critical review. *Environ. Sci. Technol.* **2018**, *52*, 5027–5047. [[CrossRef](#)]
44. Hossain, M.K.; Strezov, V.; Chan, K.Y.; Nelson, P.F. Agronomic properties of wastewater sludge biochar and bioavailability of metals in production of cherry tomato (*Lycopersicon esculentum*). *Chemosphere* **2010**, *78*, 1167–1171. [[CrossRef](#)]
45. Zielińska, A.; Oleszczuk, P.; Charmas, B.; Skubiszewska-Zięba, J.; Pasieczna-Patkowska, S. Effect of sewage sludge properties on the biochar characteristic. *J. Anal. Appl. Pyrolysis* **2015**, *112*, 201–213. [[CrossRef](#)]
46. Jones, J.M.; Darvell, L.I.; Bridgeman, T.G.; Pourkashanian, M.; Williams, A. An investigation of the thermal and catalytic behaviour of potassium in biomass combustion. *Proc. Combust. Inst.* **2007**, *31*, 1955–1963. [[CrossRef](#)]
47. Hossain, M.K.; Strezov, V.; Chan, K.Y.; Ziolkowski, A.; Nelson, P.F. Influence of pyrolysis temperature on production and nutrient properties of wastewater sludge biochar. *J. Environ. Manag.* **2011**, *92*, 223–228. [[CrossRef](#)]
48. Waqas, M.; Li, G.; Khan, S.; Shamshad, I.; Reid, B.J.; Qamar, Z.; Chao, C. Application of sewage sludge and sewage sludge biochar to reduce polycyclic aromatic hydrocarbons (PAH) and potentially toxic elements (PTE) accumulation in tomato. *Environ. Sci. Pollut. Res.* **2015**, *22*, 12114–12123. [[CrossRef](#)]